Controlled Synthesis of Small Water-Soluble Hybrid Gold Nanoparticles: An Optimized Strategy for Stable Nano-Dispersion and Towards Cellular Uptake

Tracy Bouyon Yenda, Carine Jiguet-Jiglaire, Imene Khichane, Quentin Gobert, Rathinasabapathi Prabhakaran, Alexandre de Nonneville, Thierry Djenizian, Sébastien Salas, Frédéric Dallemer

frontiers in Mechanical Engineering

ORIGINAL RESEARCH
published: 22 March 2022
doi: 10.3389/fmech.2022.824837

Controlled Synthesis of Small Water-Soluble Hybrid Gold Nanoparticles: An Optimized Strategy for Stable Nano-Dispersion and Towards Cellular Uptake

*Tracy Bouyon Yenda[1], Carine Jiguet-Jiglaire[2,3], Imene Khichane[1], Quentin Gobert[1], Rathinasabapathi Prabhakaran[1,4], Alexandre De Nonneville[5], Thierry Djenizian[6,7], Sébastien Salas[5] and Frédéric Dallemer[1]**

[1]MADIREL AMU-CNRS UMR7246 Aix Marseille Université, Marseille, France, [2]Institut of Neurophysiology INP AMU-CNRS Aix Marseille Université, Marseille, France, [3]Department of Anatomopathology, CHU Timone, AP-HM Aix Marseille Université, Marseille, France, [4]Department of Chemistry, Bharathiar University, Coimbatore, India, [5]Medical Oncology Unit, CHU Timone Adulte, AP-HM Aix Marseille Université, Marseille, France, [6]Center of Microelectronics in Provence, Flexible Electronics Department, Mines Saint-Etienne, Gardanne, France, [7]Center of Physical-Chemical Methods of Research and Analysis, Al-Farabi Kazakh National University, Almaty, Kazakhstan

OPEN ACCESS

Edited by:
Machrafi Hatim,
University of Liège, Belgium

Reviewed by:
Idris Yazgan,
Kastamonu University, Turkey
Essam Ibrahim,
King Khalid University, Saudi Arabia

***Correspondence:**
Frédéric Dallemer
frederic.dallemer@univ-amu.fr

Specialty section:
This article was submitted to Micro- and Nanoelectromechanical Systems, a section of the journal Frontiers in Mechanical Engineering

Received: *29 November 2021*
Accepted: *14 February 2022*
Published: *22 March 2022*

Citation:
Bouyon Yenda T, Jiguet-Jiglaire C, Khichane I, Gobert Q, Prabhakaran R, De Nonneville A, Djenizian T, Salas S and Dallemer F (2022) Controlled Synthesis of Small Water-Soluble Hybrid Gold Nanoparticles: An Optimized Strategy for Stable Nano-Dispersion and Towards Cellular Uptake. Front. Mech. Eng 8:824837. doi: 10.3389/fmech.2022.824837

The development of effective drug delivery systems is one of the major challenges in the fight against cancer. Gold nanoparticles could effectively harness cancer therapies by improving their potency while reducing toxic side effects. In this work, we describe a high-yield one-step synthesis of small water-soluble gold nanoparticles (AuNPs). Efficient purification was monitored, and discrete structure was fully characterized by combining molecular analytical technics (UV-visible and NMR spectroscopies) and solid-state analyses (thermal gravimetric analysis and transmission electron microscopy). These AuNPs have good dispersibility in various biocompatible media and can be used without any additives. Preliminary study with *in vitro* treatment of IB115 human cancer cells showed massive cellular uptake associated to moderate intrinsic cytotoxicity. The high control of the synthesis and the small size of these AuNPs are offering fine surface properties control, crucial for challenging biological nano-dispersion issues. Thus, limitation of the agglomeration of nanoparticles and improvement of interaction with the surface of cell should open new leads for vectorization of drugs or imaging probes for diagnosis.

Keywords: hybrid gold nanoparticles, *para*-hydroxybenzenethiol, chemical characterizations, nano-dispersion, cytotoxicity, cellular uptake

INTRODUCTION

Cancer is the second leading cause of death in the United States and in Europe (Bray et al., 2018; Siegel et al., 2018). Despite considerable improvements in cancer therapies, new tools to fight this disease are still dramatically needed (Collins and Workman, 2006; Lazo, 2010; Petrocca and Lieberman, 2011). Gold nanoparticles (AuNPs) hold promise for overcoming several limitations of conventional cytotoxic drugs or new active biomolecules such as lack of solubility in water leading

to the use of toxic solvents (Untch et al., 2016), non-specific biodistribution or low therapeutic index leading to damage to healthy tissues (Lazo, 2010; Petrocca and Lieberman, 2011; Untch et al., 2016), or development of drug resistance mechanisms via efflux pumps (Da Silva et al., 2017). They are offering potential new leads, especially for cancer treatments (Brown et al., 2010; Chanda et al., 2010; Wang et al., 2010; Riley et al., 2019; Yu et al., 2020). Therefore, the development of clean and efficient processes to produce these nanoparticles is a key challenge. The high specific surface offered by the nanoparticles gives them the possibility to interact with a high number of molecules and bio-surfaces. The ability to finely tune the chemical properties of the organic layer at the interface of hybrid metallic/organic AuNPs should be critical for controlling their specific interactions with organs, cells and active drugs. Development of efficient synthesis, ready for industrial scale-up, to achieve very high purity and control at the molecular scale is mandatory. A large range of methods have been developed for the preparation of aqueous gold nanoparticles (Frens, 1973; Brust et al., 1994; Brust et al., 1995; Kimling et al., 2006), among them, bottom-up chemical syntheses based on the reduction of Au (+III) salts are prone to a better control. Most convenient reducing agents are borohydride salts and citrate salts. The former is used for the generation of smaller AuNPs, the later tends to deliver larger ones with size exceeding 5 nm. Larson-Smith and co-workers used citrate to prepare 12 nm sized AuNPs, stabilized in water by using non-ionic polymers, polyethylene glycols PEG (Larson-Smith and Pozzo, 2012). A typical approach to get smaller water soluble AuNPs is to conduct biphasic syntheses, with extraction of the final compounds to the aqueous phase. Gittins and co-workers prepared tetraoctylammonium stabilized AuNPs in biphasic toluene/water solvent mixture, involving an ammoniumpyridine phase transfer agent (Park et al., 2009). The AuNPs of size 5.5 nm are dispersed in basic solution. Ju-Nam and co-workers developed thioacetylalkyltriphenylphosphonium ligands to form and extract AuNPs, from the biphasic solution, leading to more stable nanoparticles, sized from 5 to 10 nm (Ju-Nam et al., 2008). Major drawback of the biphasic synthesis is the toxicity related to residues of organic solvents and remaining excess of ammonium or phosphonium phase transfer agents or ligands, difficult to dispose of (Goia and Matijević, 1998; Li et al., 2020). Furthermore, the ionic strength of these AuNPs reinforces their colloidal behavior, highly sensitive to the operating conditions (Turkevich et al., 1951; Yonezawa et al., 1997). Monophasic synthesis has been conducted in methanol/water solvent mixture. Chen and co-workers used mercaptosuccinic acid to get small sized AuNPs of 1–3 nm, under basic conditions. Hussain and co-workers prepared AuNPs of size 3.5 nm in water, in the presence of weakly bounding hydrazine ligand and addition of polymeric starch and ethylene glycol to allow dispersion, but these AuNPs were prone to agglomerate (Tajammul Hussain et al., 2008). Recently, a more versatile way to get water dispersible AuNPs is introducing dispersive agents, mainly non-ionic PEG or zwitterionic polymers (Smith et al., 2013; Liu et al., 2014; Masse et al., 2019; Hussain et al., 2020; Wei et al., 2021), but leading to dynamic systems with a variable composition, difficult to control and stabilize.

The development and widespread of AuNPs applications have led to new strategies for the treatment and diagnosis of cancer and other diseases (Bastús et al., 2009; Fent et al., 2009; Chanda et al., 2010; Viator et al., 2010; Núñez et al., 2014) such as *in vivo* delivery of either therapeutic biomolecules or chemical drugs (Brown et al., 2010). Nevertheless, AuNPs represent actually a large range of chemical compounds, related to variations in physical and chemical properties, as their size, surface state, and properties of the interface layer that is usually very scarcely characterized (Shaltiel et al., 2019; Sokolowska et al., 2019; Locarno et al., 2021). This large diversity has a significant impact on the biological properties and potential applications of each type of AuNPs. Thus, we report in this paper an efficient one-step synthesis of 3.9 nm hybrid water soluble AuNPs. The small size limits the deviation of chemical composition toward a discrete molecule-like compound. That should also enhance cellular penetration in high concentration. The reported controlled purification process and specific characterizations based on molecular analytical technics (UV-visible and NMR spectroscopies) and solid-state analyses (TGA, TEM) are leading to discrete nanoparticles offering controlled properties. Cellular uptake and intrinsic cytotoxicity were preliminary assessed by direct *in vitro* treatment of IB115 cancer cells.

MATERIALS AND METHODS

Physical Measurements and Materials

Tetrachloroauric acid trihydrate ($HAuCl_4$-$3H_2O$), sodium borohydride ($NaBH_4$), *para*-hydroxybenzenethiol (HO-C_4H_4-SH), sodium hydroxide (NaOH), hydrochloric acid (HCl), ethanol (C_2H_5OH), diethyl ether ($(C_2H_5)_2O$), sodium chloride (NaCl), Pluronic F127 were purchased from Aldrich, deuterium oxide (D_2O) was purchased from Cambridge Isotope Laboratories, and used as received. For the preparation of aqueous solutions, Nanopure water (ρ >18MΩ) was produced with a Purelab UHQ NANOpure water system. Centrifugation was run at 12,000 rpm for 15 min. Dialysis was performed with 10 ml X12 Float-A-lyzer G2-8-10 KDa membrane from Spectrum Europe BV.

Transmission electron microscopy (TEM) images were obtained on a JEOL 1400 transmission electron microscope, JEOL Ltd., Tokyo, Japan. TEM samples were prepared by placing 5 μL of gold nanoparticle solution on a 300 mesh carbon-coated copper grid and allowing the solution to stand for 5 min. Excess solution was removed carefully and the grid was allowed to dry for an additional 5 min. The average size and size distribution of the synthesized gold nanoparticles were determined by analysis of TEM images using image processing software Adobe Photoshop and ImageJ.

The pH of basic aqueous solutions is controlled using Mettler Toledo Five pH-meter, daily calibrated using buffer solutions certipur at pH = 7 and pH = 10.

The absorption measurements were carried out using Varian Cary 300 scan win UV–Vis spectrophotometer in the double beam mode with 1 ml of gold nanoparticle solutions.

Proton nuclear magnetic resonance ^{1}H NMR spectra were recorded on a Bruker AC-400 NMR spectrometer at 14 g.L^{-1} concentration.

Thermal gravimetric analysis (TGA), typically based on a 8 mg sample in a platinum pot, was performed on a TG/TA Q500 analyzer (Texas Instruments, Inc.) under a Ar atmosphere (flow rate 40 ml/min) and ramp: 2°c/min from 30 to 800°C.

Quality-control materials –duplicates, spikes and instrument-calibration controls– were within appropriate ranges.

Synthesis and Purification of AuNPs

$HAuCl_4.3H_2O$ (150 mg) was dissolved in 44 ml of a 5×10^{-3} M NaOH solution in a 250 ml flask under argon atmosphere. A solution of *para*-hydroxybenzenethiol (84 mg) in 7 ml of a 0.2 M NaOH solution was added and the mixture was stirred, coloration turned from pale to dark yellow. The reaction mixture was stirred at 0°C. After 10 min, 5 ml of a $NaBH_4$ aqueous solution (145 mg) was slowly added. The solution turned to purple. The reaction mixture was stirred for 3 h. The aqueous phase was eliminated under reduced pressure at 40°C. The crude product was washed with diethyl ether and acetonitrile, then dried under inert atmosphere. 440 mg of a purple powder was obtained.

The solution of washed AuNPs in 10 ml nanopure H_2O was purified by dialysis for 8 h. Dialysate solution was evaporated under reduced pressure. After drying under inert atmosphere, 87 mg of a purple powder was obtained (isolated yield of 90%).

Estimation of the Mean Composition of AuNPs

The mean diameter of the AuNPs (3.8 nm estimated by TEM) is alignment of 7 Au atoms (according to the size of metallic gold in close packing). That is corresponding to a close packing of 920 Au atoms.

The mass of organics is representing 22% of the total mass of AuNPs (TGA), corresponding close to 53,000 g mol^{-1} for this organic layer. That represents a mean packing of 360 grafted ligands of mean formula S-C_6H_4-ONa.

Solubility Study

The nanoparticle solutions are prepared by dilution of dried AuNPs at the specified concentration in the aqueous media (nanopure water; basic NaOH solutions controlled at pH = 7, pH = 10 or pH = 12 ± 0.1; mixtures of ethanol in nanopure water at 0.5, 1, 5, 10 and 12.5% of ethanol). After centrifugation (excepted in specified experiments), the maximal absorbance is compared to the mass or molar concentration of AuNPs.

Cell Culture

IB115 cell line was obtained from Institut Bergonié, France (Lagarde et al., 2015). 3T3 cells were cultured in DMEM (Gibco). IB115 cells were cultured in RPMI 1640 (Gibco). Both cell lines were supplemented with 10% fetal bovine serum (LifeTechnologies), 50 U/mL penicillin, 50 mg/ml streptomycin (Life Technologies) and 1 mM sodium pyruvate (LifeTechnologies). Cells were maintained at 37 °C under a 5% CO_2 atmosphere.

Cytotoxicity Assay and Cellular Uptake Evaluation

The cytotoxicity and cellular uptake experiments were performed as follows: the day before treatment, 20,000 cells in 400 ml of culture media were deposited in a 24-well plate. For cytotoxicity assay, AuNPs solutions (0.1, 10 and 100 nM final concentration in the culture media) and solvents were evaluated on IB115 and 3T3 cell lines. The cells were exposed to 20 ml of the solvents (excepted for water) or nanoparticle-solutions for 24 h or 72 h before performing an MTT (3-[4,5-dimethylthiazol-2-yl]-2,5-diphenyl tetrazolium bromide) assay (Sigma-Aldrich) as described by the manufacturer. Three independent experiments were performed, each in triplicate. The error bars represent the standard deviation of the mean (n = 3).

The solvents are solution in nanopure water of bovine serum albumin (2.5 and 5%), mixture of ethanol in nanopure water (0.5, 1, 5, 10 and 12.5% of ethanol), solution in nanopure water of glucose (2, 2.5, 3, 4 and 5%), sodium chloride solution in nanopure water (0.9%), nanopure water at the specified volume percentage (1, 5, 10, 15 and 20% of the culture media).

The nanoparticle solutions are prepared by dilution of dried AuNPs at 0.5 g.L^{-1} in 0.9% NaCl solution in the presence of Pluronic F127, at the same molar concentration than AuNPs, then diluted by nanopure water for preparation of 20 ml of solution at the targeted concentration.

Cellular uptake was evaluated on IB115 cells after treatment by the nanoparticle solution at the final concentration of 100 nM AuNPs in the culture media, for 3 days. Transmission Electronic Microscopy imaging was performed to visualize late endocytosis vesicles.

TEM Cell Imaging

Cells were washed three times, fixed by 2.5% glutaraldehyde in 0.1 M cacodylate buffer, pH 7.4, postfixed in osmium tetroxide 1%. Cells were then scraped and centrifuged. The pellets of cells were dehydrated in graded alcohol solutions and embedded in SPURR low-viscosity medium. Ultrathin sections (50–60 nm) were counterstained by uranyl acetate and lead citrate before observation with a JEOL JEM1400 electron microscope at 80 kV. Images were obtained with MegaView III camera (Soft Imaging System).

Quality-control materials –duplicates, spikes and instrument-calibration controls– were within appropriate ranges.

RESULTS AND DISCUSSION

Synthesis and Purification of AuNPs

The reported preparation of small water soluble AuNPs is involving the reduction of Au (+III) salt by sodium borohydride $NaBH_4$, from protocols by Brust and co-workers, either in biphasic solution (Brust et al., 1994) or in methanolic solutions (Brust et al., 1995). The former route is less convenient

TABLE 1 | Comparison of the UV-visible maximum absorption along the purification process, in pure water (ε_1 weight specific absorbance; ε_2 estimated molar specific absorbance).

Sample	Initial conc. ($g.L^{-1}$)	λ_{max} (nm)	Absorbance	ε_1 ($L.g^{-1}.cm^{-1}$)	ε_2 ($L.Mol^{-1}.cm^{-1}$)
Crude AuNPs	2.57	550	3.44	2.68	6.22×10^5
Washed AuNPs	1.93	549	1.62	1.68	3.42×10^5
Dialyzed AuNPs	0.447	547	1.08	4.83	9.83×10^5

to control and the phase transfer agent or hydrophilic ligand could introduce noxious side effects. The later one is convenient, but the use of toxic methanol could limit biological uses as the organic interface layer of the AuNPs is prone to high solvation effects, strongly trapping residual methanol molecules. Furthermore, a strongly basic treatment is needed in order to increase water solubility of the generated aqueous methanolic AuNPs.

We developed here a direct synthesis in water, without the use of any organic cosolvent or phase transfer additive. Reduction of the gold salt is conducted in the presence of thiols, as they are generating the strongest interactions with gold surface (Brust et al., 1995; Price and Whetten, 2005; Price and Whetten, 2006; Lopez-Acevedo et al., 2009; Thakur and Gathania, 2015), crucial to secure the stability of the generated nanoparticles. These strong interactions should also promote a better control of the organic interface layer, less prone to dynamic rearrangements and exchanges. We selected the *para*-hydroxybenzenethiol, providing a phenol function for improved water solubility and offering a large potential for intermolecular binding interactions. The pH of the starting material solutions is controlled, in order to prevent the formation of largest insoluble dark blue gold nanoparticles.

Excess of thiol molecules are removed after drying the crude mixture of AuNPs and washing it with diethyl ether and acetonitrile. Purification process is completed by dialysis, using a membrane of narrow porosity. After water evaporation, a stable purple powder is obtained, convenient for long-term storage.

The purification process is monitored by the following up of the successive weight losses and quantitative molecular analyses. The effective elimination of the excess of starting materials and by-products is a critical step to achieve, in order to control the actual composition of the nanoparticles and to prevent them from releasing small molecules with adverse effects.

Characterization of AuNPs

The dark coloration of the AuNPs is resulting from a strong adsorption band at 550 nm in neutral water or at 530 nm in basic water (in **Supplementary Figure S1**, see **Supplementary Material**). Attributed to the surface plasmon resonance SPR, the wavelength and intensity of this maximum absorption is in good agreement with the formation of spherical AuNPs exceeding few nm of size (Tréguer-Delapierre et al., 2008).

After repeated washing and dialysis operations, the AuNPs sample is topping a maximum specific adsorption, reaching the highest level of purification (**Table 1**).

Liquid 1H-NMR spectroscopy is an effective tool for characterization of the organic layer constitutive of the hybrid AuNPs. The free thiol is showing a characteristic thin doublet of doublets peak pattern at the expected aromatic range of chemical shifts (**Figure 1**).

The purification steps are clearly leading to the disappearance of this aromatic thin peak pattern, exhibiting the broad pattern of aromatic peaks attributed to the thiols bound to the gold surface (**Figure 2**). The washing process has a moderate effect for elimination of the exceeding thiols. On the other hand, the dialysis has a dramatic effect, fully extracting the excess of free thiols. The full range ^{1}H-NMR spectrum of dialyzed AuNPs can be found in **Supplementary Figure S2A**.

In comparison to the free thiol, aromatic proton peaks are considerably broader in the hybrid AuNPs (**Figure 1**). The binding of the thiol molecules is reducing their mobility and the isotropy of their movements, leading to a broadening of the peaks. Furthermore, a strong nuclear coupling between the protons and the gold surface should be reinforced through the aromatic electronic conjugation, enhancing scalar couplings. The presence of several shifted multiplets, generating a fine structure over the broad peaks, should be related to remotely bound thiols, on different relative locations at the surface of gold particles. The integration of the NMR peaks relative to the aromatic protons of grafted thiols shows the 1:1 ratio related to the para-substitution pattern of the thiol (**Supplementary Figure S2B**). This is a clear indication that their chemical integrity has been preserved.

Transmission Electronic microscopy is showing small AuNPs of 3.9 ± 0.3 nm size, with a narrow size distribution (**Figures 3**, **4**), in the size range of biomacromolecules like small proteins. According to the mean diameter of the gold core, the estimation for the total number of gold atoms is 920, including 360 gold atoms exposed at the surface, assuming a face-centered cubic close packed system.

The thermogravimetric analysis of the AuNPs is indicating a total weight loss of 22% from 150 to 500°C, with stabilization of the weight at higher temperature (in **Supplementary Figure S3**). The final product is gold yellow. The weight loss develops in two steps. The first one occurred at 200–250°C, the second one between 250 and 450°C. Under the same analytical conditions, most of the free thiol sample weight is lost at much lower temperature, from 50 to 150°C. These results are showing that the thiol ligands are strongly embedded onto the gold surface. The outer layer of thiols less strongly interacting with the gold atoms, is lost at the lower temperature range, then the inner layer more strongly bounded to the surface is lost at higher temperature.

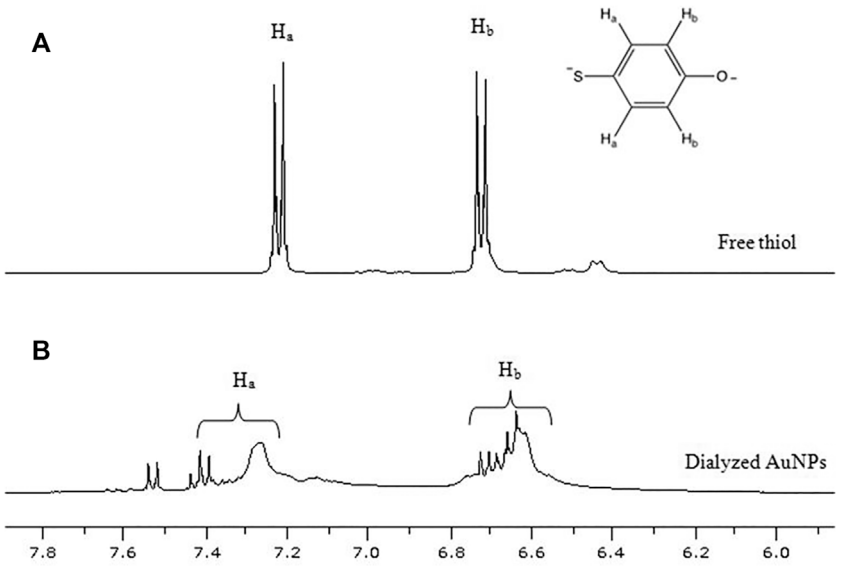

FIGURE 1 | Comparison of ^{1}H-NMR spectra in the aromatic proton chemical shift range: upper **(A)** free *para*-hydroxybenzenethiol (in D_2O/NaOH, pH 12); lower **(B)** AuNPs in D_2O.

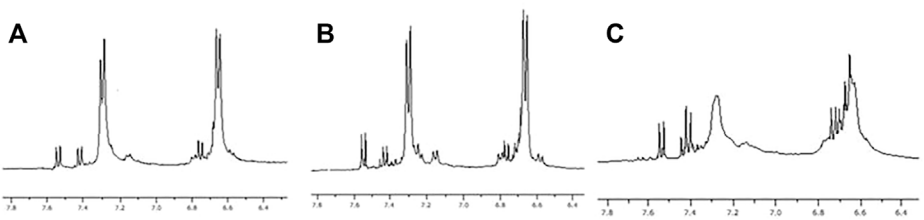

FIGURE 2 | Comparison of ^{1}H-NMR spectra in the aromatic proton chemical shift range: left **(A)** crude AuNPs; center **(B)** washed AuNPs; right **(C)** dialyzed AuNPs.

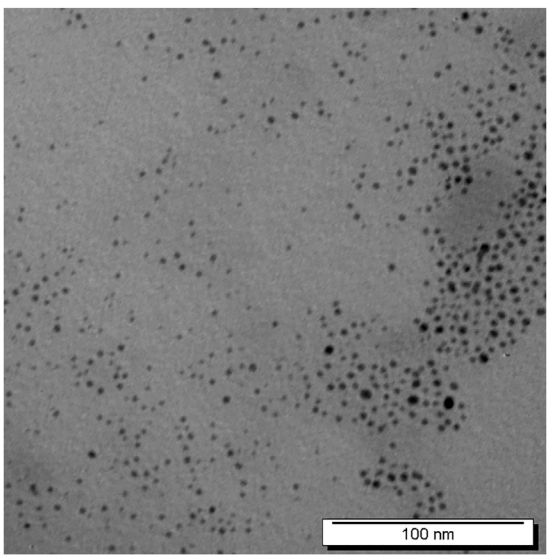

FIGURE 3 | TEM image of AuNPs.

That agrees with the NMR spectra exhibiting a double pattern for the aromatic protons of AuNPs, either as broad peaks for thiols strongly coupled to the surface or a fine structure of multiplets for the more remote ones. According to the mean size of the gold core and the successive weight losses of thiols, the mean composition for the AuNPs is $Au_{920}(S\text{-}C_6H_4\text{-}ONa)_{360}$ including a first layer of 140 thiols closely interacting with the gold core and a outer layer of 220 thiols.

Solubility of AuNPs in Aqueous Solutions

Highly divided materials as nanoparticles tend to agglomerate, being less available for interactions with biological systems. Additionally, water is significantly reactive with metallic systems, as a weak acid, a weak base, a moderate oxidant and exhibits a strong dissociative effect. This is a severe limitation for the practical use of nanoparticles; such systems tend to experience stability issues and poor bioavailability. The most sensitive method for monitoring degradation or aggregation of nanoparticles relies on assessment of the specific SPR absorbance.

The prepared AuNPs have a good solubility, exceeding 1 g L^{-1} in water, with no need to add any strong base. The estimation for

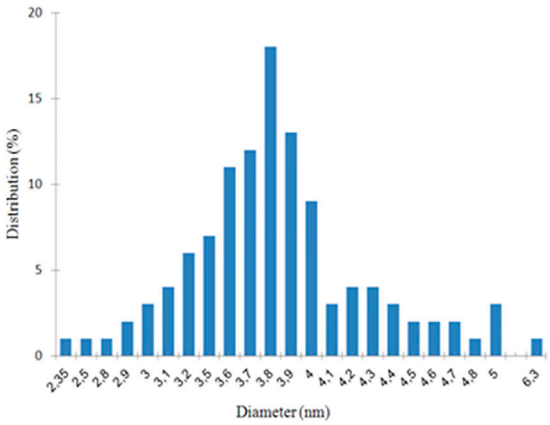

FIGURE 4 | Size distribution histogram of AuNPs.

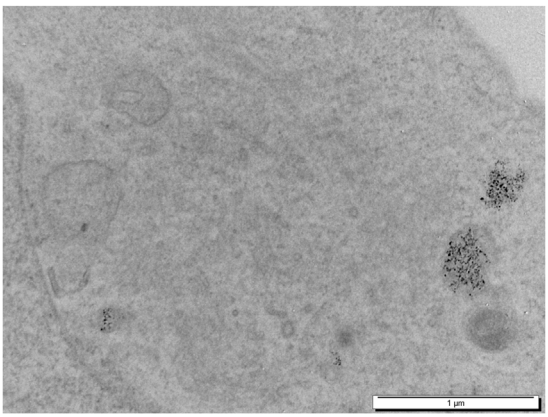

FIGURE 5 | Time and dose dependence of cytotoxicity on IB115 sarcoma cells line. D1 is after 1 day and D3 is after 3 days.

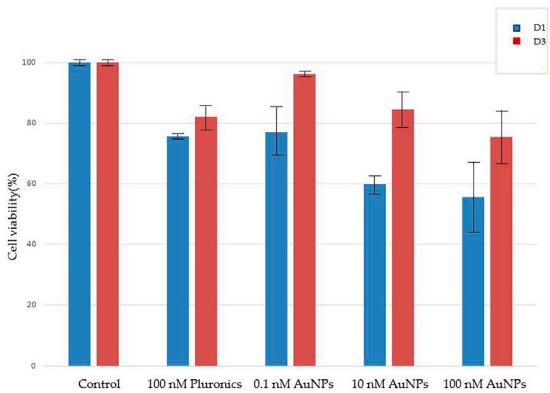

FIGURE 6 | TEM image of IB115 cells 3 days after AuNPs exposure.

the maximum weight specific absorbance ε_1 is 2 L g^{-1} cm^{-1}, with no variation after the centrifugation step (in **Supplementary Table S1**). The estimated maximum molar specific absorbance ε_2 is 4.10^5 L $mol^{-1}.cm^{-1}$, in good agreement with the expected value for SPR bands (Tréguer-Delapierre et al., 2008). Their stability in water is adequate, with no sensible decrease of the absorbance after up to 8 days, at the concentration of 0.1 g/L^{-1}. There is no evidence for any agglomeration in solution. Theses AuNPs offer a maximum nano-dispersion and a maximum bioavailability.

The increase of pH up to 12 has a significant effect on the SPR absorption with a 20 nm shift of the maximum wavelength as well as an increase of its intensity. That should be related to the full deprotonation of the hydroxybenzene groups on the thiol ligands, leading to a significant modification of the organic layer electronic density.

Solubility in biocompatible ethanol/water mixtures is in the same concentration range of 0.1 g L^{-1}, and the maximum specific absorbance ε_1 remains close to 2 L g^{-1} cm^{-1} (in **Supplementary Table S2**).

Addition of 0.9% NaCl salt decreases the solubility of AuNPs down to 0.05 g/L^{-1}. Higher solubility up to 0.38 g/L^{-1} is obtained in the presence of the non-ionic surfactant F127 Pluronics.

Cytotoxicity Assessment and Cellular Uptake

The purpose of the highly controlled synthesis for AuNPs is to develop effective systems that could circumvent the delivery barriers faced into solid tumors, up to the cell and the nucleus. The first things to check out are therefore cytotoxicity and cellular uptake. We selected the IB115 human sarcoma cell line, responsible for accessible and aggressive solid tumors, for *in vitro* preliminary evaluation. Assessment of the cytotoxicity of solvent mixtures was conducted *in vitro* to determine the most appropriate one to be used for AuNPs delivery. Introduction in the culture medium of less than 5% of pure water, ethanol or 0.9% NaCl solution had moderate impact on cells survival. Evaluation of AuNPs cytotoxicity, based on MTT assays, was conducted at days 1 and 3. The nanoparticles were delivered at 3 different concentrations in a 0.9% NaCl solution with Pluronic F127 surfactant (**Figure 5**).

Pluronic F127 alone induced a moderate mortality of 24 ± 1% of the cells at day 1 and 18 ± 4% at day 3. Addition of AuNPs altered cell death at day 1–23 ± 8%, 40 ± 13% and 44 ± 12% at the doses of 0.1, 10 and 100 nM, respectively. The same dose effect was observed at day 3 but at a lower level (4 ± 1%, 16 ± 6% and 25 ± 9% % at the doses of 0.1, 10 and 100 nM, respectively). The initial mortality after day 1 could be related to the sensitivity of the cells line, as the control cytotoxicity of the aqueous media show it, in **Supplementary Figure S4A**.

We observed only low AuNPs toxicity in a control study on a non-tumor cell line such as 3T3 (normal mouse embryonary fibroblast), exposed in **Supplementary Figure S4B**. Pluronic F127 showed similar results to those obtained with the tumor cell line, with moderate cytotoxicity, but when combined with AuNPs in the nanoparticle solutions, we observed again a decreased low cyctotoxicity.

Cellular uptake of AuNPs by IB115 cells was estimated by electronic microscopy imaging. Massive cellular uptakes were observed 3 days after treatment, with evidence for numerous late endocytose vesicles, full packed with discrete non-agglomerated AuNPs (**Figure 6**).

CONCLUSION

Small AuNPs of 3.9 nm of mean size were synthesized in high-yield, by reducing Au (+III) salt with borohydride in the presence of *para*-hydroxybenzenethiol, directly in basic aqueous solution without organic solvents or additives. Extensive purification including dialysis led to well-defined AuNPs embedded in multilayered thiol ligands, fully characterized by TEM, TGA, UV-visible and NMR spectroscopies. NMR and TGA data suggest that all thiol ligands are stabilizing the gold core, structured in a first layer of thiols closely connected to gold atoms, and a second layer, more remotely connected to the gold surface. These AuNPs are discrete hybrid compounds with the mean composition $Au_{920}(S\text{-}C_6H_4\text{-}ONa)_{360}$, without dynamic exchange of ligands at the NMR time scale, and so with defined surface properties. Due to the strong binding of the thiol ligands, these AuNPs are stable, with no agglomeration in aqueous media. The control of the organic to metal ratio is expected to govern the hydrophilic to lipophilic balance of the nanoparticles. It should be an important factor to control aqueous dispersion of the hybrid AuNPs in water and their interactions with cellular membranes. First *in vitro* experiments showed a low intrinsic toxicity and a high cellular uptake. The preliminary results suggest that these hybrid AuNPs could be relevant as delivery vectors for cancer therapy or diagnosis applications by offering a better control of their composition and the possibility to finely tune their surface properties. These smaller nanoparticles should lead to a new approach for nano-transportation by targeting the cellular penetration issues.

DATA AVAILABILITY STATEMENT

The original contributions presented in the study are included in the article/**Supplementary Material**, further inquiries can be directed to the corresponding author.

AUTHOR CONTRIBUTIONS

FD, SS, and TD designed the work, FD, SS, RP, and CJ-J conceived the experiments, TB, CJ-J, IK, and QG conducted the experiments and the acquisition of the analysis, FD, CJ-J, SS, TB, and QG analysed the results, AD substantially reviewed the draft, FD drafted the work and revision of it. All authors reviewed the manuscript.

FUNDING

The research was funded by the Excellence Initiative of Aix-Marseille University–A*Midex, a French "Investissements d'Avenir" program, grant number A-M-AAP-ID-17-67-170301-11.58.

ACKNOWLEDGMENTS

The authors are grateful for helpful discussions and precious technical supports, related to TEM imaging and samples preparations, to Dr. Joel Courageot and Dr. Alexandre Altie, Central Supporting Service for Electronic Microscopies, Faculty of Medicine, La Timone campus, Aix-Marseille Université.

SUPPLEMENTARY MATERIAL

The Supplementary Material for this article can be found online at: https://www.frontiersin.org/articles/10.3389/fmech.2022.824837/full#supplementary-material

REFERENCES

Bastús, N. G., Sánchez-Tilló, E., Pujals, S., Farrera, C., López, C., Giralt, E., et al. (2009). Homogeneous Conjugation of Peptides onto Gold Nanoparticles Enhances Macrophage Response. *ACS Nano* 3 (6), 1335–1344. doi:10.1021/nn8008273

Bray, F., Ferlay, J., Soerjomataram, I., Siegel, R. L., Torre, L. A., and Jemal, A. (2018). Global Cancer Statistics 2018: GLOBOCAN Estimates of Incidence and Mortality Worldwide for 36 Cancers in 185 Countries. *CA: A Cancer J. Clin.* 68 (6), 394–424. doi:10.3322/caac.21492

Brown, S. D., Nativo, P., Smith, J.-A., Stirling, D., Edwards, P. R., Venugopal, B., et al. (2010). Gold Nanoparticles for the Improved Anticancer Drug Delivery of the Active Component of Oxaliplatin. *J. Am. Chem. Soc.* 132 (13), 4678–4684. doi:10.1021/ja908117a

Brust, M., Walker, M., Bethell, D., Schiffrin, D. J., and Whyman, R. (1994). Synthesis of Thiol-Derivatised Gold Nanoparticles in a Two-phase Liquid-Liquid System. *J. Chem. Soc. Chem. Commun.* 7, 801–802. doi:10.1039/C39940000801

Brust, M., Fink, J., Bethell, D., Schiffrin, D. J., and Kiely, C. (1995). Synthesis and Reactions of Functionalised Gold Nanoparticles. *J. Chem. Soc. Chem. Commun.* 16, 1655–1656. doi:10.1039/C39950001655

Chanda, N., Kattumuri, V., Shukla, R., Zambre, A., Katti, K., Upendran, A., et al. (2010). Bombesin Functionalized Gold Nanoparticles Show *In Vitro* and *In Vivo* Cancer Receptor Specificity. *Proc. Natl. Acad. Sci.* 107 (19), 8760–8765. doi:10.1073/pnas.1002143107

Collins, I., and Workman, P. (2006). New Approaches to Molecular Cancer Therapeutics. *Nat. Chem. Biol.* 2 (12), 689–700. doi:10.1038/nchembio840

Da Silva, C. G., Peters, G. J., Ossendorp, F., Cruz, L. J., and Cruz, L. J. (2017). The Potential of Multi-Compound Nanoparticles to Bypass Drug Resistance in Cancer. *Cancer Chemother. Pharmacol.* 80 (5), 881–894. doi:10.1007/s00280-017-3427-1

Fent, G. M., Casteel, S. W., Kim, D. Y., Kannan, R., Katti, K., Chanda, N., et al. (2009). Biodistribution of Maltose and Gum Arabic Hybrid Gold Nanoparticles after Intravenous Injection in Juvenile Swine. *Nanomed. Nanotechnol. Biol. Med.* 5 (2), 128–135. doi:10.1016/j.nano.2009.01.007

Frens, G. (1973). Controlled Nucleation for the Regulation of the Particle Size in Monodisperse Gold Suspensions. *Nat. Phys. Sci.* 241 (105), 20–22. doi:10.1038/physci241020a0

Goia, D. V., and Matijević, E. (1998). Preparation of Monodispersed Metal Particles. *New J. Chem.* 22 (11), 1203–1215. doi:10.1039/A709236I

Hussain, M. H., Abu Bakar, N. F., Mustapa, A. N., Low, K.-F., Othman, N. H., Adam, F., et al. (2020). Synthesis of Various Size Gold Nanoparticles by

Chemical Reduction Method with Different Solvent Polarity. *Nanoscale Res. Lett.* 15 (1), 140. doi:10.1186/s11671-020-03370-5

Ju-Nam, Y., Allen, D. W., Gardiner, P. H. E., and Bricklebank, N. (2008). ω-Thioacetylalkylphosphonium Salts: Precursors for the Preparation of Phosphonium-Functionalised Gold Nanoparticles. *J. Organomet. Chem.* 693 (23), 3504–3508. doi:10.1016/j.jorganchem.2008.08.009

Kimling, J., Maier, M., Okenve, B., Kotaidis, V., Ballot, H., and Plech, A. (2006). Turkevich Method for Gold Nanoparticle Synthesis Revisited. *J. Phys. Chem. B* 110 (32), 15700–15707. doi:10.1021/jp061667w

Lagarde, P., Brulard, C., Pérot, G., Mauduit, O., Delespaul, L., Neuville, A., et al. (2015). Stable Instability of Sarcoma Cell Lines Genome Despite Intra-tumoral Heterogeneity: a Genomic and Transcriptomic Study of Sarcoma Cell Lines. Austin J. *Genet. Genomic Res.* 2 (2), 1014–1022.

Larson-Smith, K., and Pozzo, D. C. (2012). Pickering Emulsions Stabilized by Nanoparticle Surfactants. *Langmuir* 28 (32), 11725–11732. doi:10.1021/la301896c

Lazo, J. S. (2010). Molecular Biology and Anticancer Drug Discovery. *Prog. Mol. Biol. Transl. Sci.* 95, 9–29. doi:10.1016/B978-0-12-385071-3.00002-2

Li, Y., Zhen, J., Tian, Q., Shen, C., Zhang, L., Yang, K., et al. (2020). One Step Synthesis of Positively Charged Gold Nanoclusters as Effective Antimicrobial Nanoagents against Multidrug-Resistant Bacteria and Biofilms. *J. Colloid Interf. Sci.* 569, 235–243. doi:10.1016/j.jcis.2020.02.084

Liu, X., Li, H., Jin, Q., and Ji, J. (2014). Surface Tailoring of Nanoparticles via Mixed-Charge Monolayers and Their Biomedical Applications. *Small* 10 (21), 4230–42. doi:10.1002/smll.201401440

Locarno, S., Bucci, R., Impresari, E., Gelmi, M. L., Pellegrino, S., and Clerici, F. (2021). Ultrashort Peptides and Gold Nanoparticles: Influence of Constrained Amino Acids on Colloidal Stability. *Front. Chem.* 9, 736519. doi:10.3389/fchem.2021.736519

Lopez-Acevedo, O., Akola, J., Whetten, R. L., Grönbeck, H., and Häkkinen, H. (2009). Structure and Bonding in the Ubiquitous Icosahedral Metallic Gold Cluster Au144(SR)60. *J. Phys. Chem. C* 113 (13), 5035–5038. doi:10.1021/jp8115098

Masse, F., Desjardins, P., Ouellette, M., Couture, C., Omar, M. M., Pernet, V., et al. (2019). Synthesis of Ultrastable Gold Nanoparticles as a New Drug Delivery System. *Molecules* 24, 2929–2945. doi:10.3390/molecules24162929

Núñez, C., Oliveira, E., García-Pardo, J., Diniz, M., Lorenzo, J., Capelo, J. L., et al. (2014). A Novel Quinoline Molecular Probe and the Derived Functionalized Gold Nanoparticles: Sensing Properties and Cytotoxicity Studies in MCF-7 Human Breast Cancer Cells. *J. Inorg. Biochem.* 137, 115–122. doi:10.1016/j.jinorgbio.2014.04.007

Park, C., Youn, H., Kim, H., Noh, T., Kook, Y. H., Oh, E. T., et al. (2009). Cyclodextrin-covered Gold Nanoparticles for Targeted Delivery of an Anti-cancer Drug. *J. Mater. Chem.* 19 (16), 2310–2315. doi:10.1039/B816209C

Petrocca, F., and Lieberman, J. (2011). Promise and Challenge of RNA Interference-Based Therapy for Cancer. *Jco* 29 (6), 747–754. doi:10.1200/jco.2009.27.6287

Price, R. C., and Whetten, R. L. (2005). All-Aromatic, Nanometer-Scale, Gold-Cluster Thiolate Complexes. *J. Am. Chem. Soc.* 127 (40), 13750–13751. doi:10.1021/ja053968+

Price, R. C., and Whetten, R. L. (2006). Raman Spectroscopy of Benzenethiolates on Nanometer-Scale Gold Clusters. *J. Phys. Chem. B* 110 (44), 22166–22171. doi:10.1021/jp062840r

Riley, R. S., June, C. H., Langer, R., and Mitchell, M. J. (2019). Delivery Technologies for Cancer Immunotherapy. *Nat. Rev. Drug Discov.* 18 (3), 175–196. doi:10.1038/s41573-018-0006-z

Shaltiel, L., Shemesh, A., Raviv, U., Barenholz, Y., and Levi-Kalisman, Y. (2019). Synthesis and Characterization of Thiolate-Protected Gold Nanoparticles of Controlled Diameter. *J. Phys. Chem. C* 123, 28486–28493. doi:10.1021/acs.jpcc.9b08817

Siegel, R. L., Miller, K. D., and Jemal, A. (2018). Cancer Statistics, 2018. *CA: A Cancer J. Clin.* 68 (1), 7–30. doi:10.3322/caac.21442

Smith, C. A., Simpson, C. A., Kim, G., Carter, C. J., and Feldheim, D. L. (2013). Gastrointestinal Bioavailability of 2.0 Nm Diameter Gold Nanoparticles. *ACS Nano* 7 (5), 3991–3996. doi:10.1021/nn305930e

Sokołowska, K., Malola, S., Lahtinen, M., Saarnio, V., Permi, P., Koskinen, K., et al. (2019). Towards Controlled Synthesis of Water-Soluble Gold Nanoclusters: Synthesis and Analysis. *J. Phys. Chem. C* 123, 2602–2612. doi:10.1021/acs.jpcc.8b11056

Tajammul Hussain, S., Iqbal, M., and Mazhar, M. (2008). Size Control Synthesis of Starch Capped-Gold Nanoparticles. *J. Nanopart. Res.* 11 (6), 1383–1391. doi:10.1007/s11051-008-9525-6

Thakur, S., and Gathania, A. K. (2015). Synthesis and Characterization of YVO4-Based Phosphor Doped with Eu3+ Ions for Display Devices. *J. Elec Mater.* 44 (10), 3444–3449. doi:10.1007/s11664-015-3884-4

Tréguer-Delapierre, M., Majimel, J., Mornet, S., Duguet, E., and Ravaine, S. (2008). Synthesis of Non-spherical Gold Nanoparticles. *Gold Bull.* 41 (2), 195–207. doi:10.1007/BF03216597

Turkevich, J., Stevenson, P. C., and Hillier, J. (1951). A Study of the Nucleation and Growth Processes in the Synthesis of Colloidal Gold. *Discuss. Faraday Soc.* 11, 55–75. doi:10.1039/DF9511100055

Untch, M., Jackisch, C., Schneeweiss, A., Conrad, B., Aktas, B., Denkert, C., et al. (2016). Nab-Paclitaxel versus Solvent-Based Paclitaxel in Neoadjuvant Chemotherapy for Early Breast Cancer (GeparSepto-GBG 69): A Randomised, Phase 3 Trial. *Lancet Oncol.* 17 (3), 345–356. doi:10.1016/S1470-2045(15)00542-2

Viator, J. A., Gupta, S., Goldschmidt, B. S., Bhattacharyya, K., Kannan, R., Shukla, R., et al. (2010). Gold Nanoparticle Mediated Detection of Prostate Cancer Cells Using Photoacoustic Flowmetry with Optical Reflectance. *J Biomed. Nanotechnol.* 6 (2), 187–191. doi:10.1166/jbn.2010.1105

Wang, B., Rosano, J. M., Cheheltani, R. e., Achary, M. P., and Kiani, M. F. (2010). Towards a Targeted Multi-Drug Delivery Approach to Improve Therapeutic Efficacy in Breast Cancer. *Expert Opin. Drug Deliv.* 7 (10), 1159–1173. doi:10.1517/17425247.2010.513968

Wei, J., Huang, X., Zhang, L., Chen, Y., Niikura, K., Mitomo, H., et al. (2021). Vesicle Formation by the Self-Assembly of Gold Nanoparticles Covered with Fluorinated Oligo(ethylene Glycol)-Terminated Ligands and its Stability in Aqueous Solution. *Langmuir* 37 (32), 9694–9700. doi:10.1021/acs.langmuir.1c00996

Yonezawa, T., Sutoh, M., and Kunitake, T. (1997). Practical Preparation of Size-Controlled Gold Nanoparticles in Water. *Chem. Lett.* 26 (7), 619–620. doi:10.1246/cl.1997.619

Yu, Y., Yang, T., and Sun, T. (2020). New Insights into the Synthesis, Toxicity and Applications of Gold Nanoparticles in CT Imaging and Treatment of Cancer. *Nanomedicine* 15 (11), 1127–1145. doi:10.2217/nnm-2019-0395

Conflict of Interest: The authors declare that the research was conducted in the absence of any commercial or financial relationships that could be construed as a potential conflict of interest.

Publisher's Note: All claims expressed in this article are solely those of the authors and do not necessarily represent those of their affiliated organizations, or those of the publisher, the editors and the reviewers. Any product that may be evaluated in this article, or claim that may be made by its manufacturer, is not guaranteed or endorsed by the publisher.